5ICEGE
5th International Conference on Earthquake Geotechnical Engineering
January 2011, 10-13 | Santiago, Chile
Paper No. SVELI

SEISMIC VULNERABILITY EVALUATION OF AN EARTHEN EMBANKMENT – A CASE STUDY

John Liao[1], Ph.D., P.E., Craig Hall[2], P.E., G.E., Scott Anderson[3], P.E.

ABSTRACT

This paper presents a case study of a seismic vulnerability evaluation of an earthen embankment which protects groundwater infiltration ponds from potential flooding from an adjacent creek. The embankment is located in the highly seismically active San Francisco Bay Area in which the probability of a magnitude 6.7 or larger earthquake over the next 30 years is forecast to be 63 percent.

To evaluate seismic vulnerability of the embankment, two analytical approaches were used: a simplified sliding block analysis and a fully nonlinear dynamic analysis. The simplified sliding block analysis considered the stability of the embankment using the limit equilibrium method and estimated the lateral displacement. Estimated post-liquefaction residual shear strengths were used for liquefiable soils in the simplified sliding block analysis. An effective-stress-based nonlinear dynamic analysis was performed using computer program FLAC (Itasca, 2008a) to evaluate the seismic response of the embankment. Unlike the simplified sliding block analysis, the fully nonlinear dynamic analysis in a coupled way modeled the occurrence of liquefaction of granular soils and lateral displacements.

In this case study, the important aspects of the models are discussed. The results of numerical analyses using the two analytical approaches are presented, and the results are interpreted to assess the seismic vulnerability of the embankment. The results of the simplified sliding block analysis and the nonlinear dynamic analysis are compared.

Keywords: Seismic Vulnerability; Earthen Embankment; Simplified Analysis; Dynamic Analysis

INTRODUCTION

Two analytical approaches of increasing complexity are generally available to evaluate seismic vulnerability of natural slopes or embankments: (1) simplified sliding block method (e.g., Makdisi and Seed, 1978; Bray and Rathje, 1998; Bray and Travasarou, 2007); and (2) fully nonlinear dynamic method. These two analytical methods were utilized in this case study to evaluate seismic vulnerability of an earthen embankment located in the seismically active San Francisco Bay Area where the probability of a magnitude 6.7 or larger earthquake over the next 30 years is forecast to be 63 percent (WGCEP, 2007).

The simplified sliding block analysis considered the stability of the embankment using the limit equilibrium method and estimated the lateral movement using the simplified Bray and Travasarou (2007) procedure. Estimated post-liquefaction residual shear strengths were used for liquefiable soils in the simplified sliding block analysis. An effective-stress-based nonlinear dynamic analysis was performed

[1] Project Engineer, Kleinfelder, Oakland, California-USA, e-mail: jliao@kleinfelder.com
[2] Senior Project Manager, Kleinfelder, Oakland, California-USA, e-mail: cahall@kleinfelder.com
[3] Principal Engineer, Kleinfelder, Sacramento, California-USA, e-mail: sanderson@kleinfelder.com

using the computer program FLAC (Itasca, 2008a) to evaluate seismic response of the embankment. Unlike the simplified sliding block analysis, the full nonlinear dynamic analysis in a coupled way modeled the occurrence of liquefaction of granular soils and lateral displacements.

METHODS OF ANALYSIS

Simplified Sliding Block Analysis

Seismic displacements of a slope or an embankment can be estimated by either a simplified sliding block analysis or a nonlinear dynamic analysis. Simplified sliding block methods have proven to be a valuable tool in evaluating seismic performance of earth dams and natural slopes (e.g., Makdisi and Seed, 1978; Bray and Travasarou, 2007; Ausilio et al., 2008). However, there is only limited literature indicating that simple sliding block methods are reliable for cases where significant strength loss from liquefaction occurs (Olson and Johnson, 2008).

Simplified sliding block methods, based on Newmark (1965) sliding block model, are widely used to assess seismic displacements in dams and embankments. These simplified methods normally fall into one of three types: (1) methods assuming a rigid sliding block assumptions (Lin and Whitman, 1986; Ambraseys and Menu 1988; Yegian et al, 1991); (2) methods assuming a decoupled stick-slip deformable sliding block model (Makdisi and Seed, 1978); and (3) methods assuming a coupled stick-slip deformable sliding block model (Bray and Travasarou, 2007).

Compared to other methods, one of the important advantages of the simplified Bray and Travasarou method is that its nonlinear coupled stick-slip deformable sliding block model offers a more realistic representation of dynamic response of an earth structure by accounting for the deformability of the sliding mass and by considering the simultaneous occurrence of its nonlinear dynamic response and periodic sliding episodes.

Bray and Travasarou found that their procedure provides estimates of seismic displacements that are generally consistent with documented cases of earth dam and solid-waste landfill performance.

Due to the inherent limitations of the simplified sliding block method, the handling of soil liquefaction in practice is usually divided into three decoupled steps: (1) triggering evaluation of soil liquefaction, (2) static slope stability evaluation, and (3) lateral deformation evaluation. While this sequential process is convenient and practical to implement, it has disadvantages, particularly its inability to model the build-up and dissipation of the excess pore pressure.

Fully Nonlinear Dynamic Analysis

The occurrence of soil liquefaction is an important factor to seismic response of an embankment. It is generally accepted that, if soil liquefaction is not triggered, the deformations only accumulate during the shaking and are often relatively small. However, if liquefaction is triggered, much larger displacements and possibly flow failure may occur. Occurrence of numerous flow failures have been observed following liquefaction (Ishihara, 1984; Seed, 1987).

The time-history based nonlinear dynamic analysis with built-in models of describing liquefaction behavior of cohesionless soils can overcome some of the limitations of the simplified sliding block analysis. Constitutive models are available that account for pore-pressure build-up and dissipation,

ranging from total-stress models (e.g., the UBCTOT model (Beaty and Byrne, 2000)), to simple effective-stress coupling models (e.g., the Finn model (Byrne, 1991)), and to more comprehensive constitutive models (e.g., the UBCSand model (Byrne et al. (1995)). These models account for the buildup and dissipation of pore water pressures and the timing of liquefaction, which can be important when assessing seismic slope displacements.

SUBJECT EARTHEN EMBANKMENT

The subject embankment is located in the seismically active San Francisco Bay Area and in close proximity to the Hayward Fault (Figure 1).

The embankment was engineered and constructed by the U.S. Army Corps of Engineers in the 1970s. It is about 600 feet long, 24 feet high on the creek side and 50 feet high on the pond side. The embankment separates two infiltration ponds from the creek that runs parallel to the embankment. The crest of the embankment is relatively flat and varies in width between 80 and 170 feet. The embankment slopes down to the creek at an inclination of approximately 2 horizontal to 1 vertical and slopes down to the pond at an inclination of about 2.5 horizontal to 1 vertical.

The subsurface condition along the embankment generally consists of up to 17 feet of levee fill material overlying alluvium sand and gravel with varying amounts of clay and silt. In general, the levee fill material consists of medium dense silty sand with gravel. Underlying the levee fill material are medium dense sand and gravel. Figure 2 presents the generalized soil profile with estimated shear wave velocities based on correlation with SPT blow counts. Figure 3 illustrates the generalized cross section.

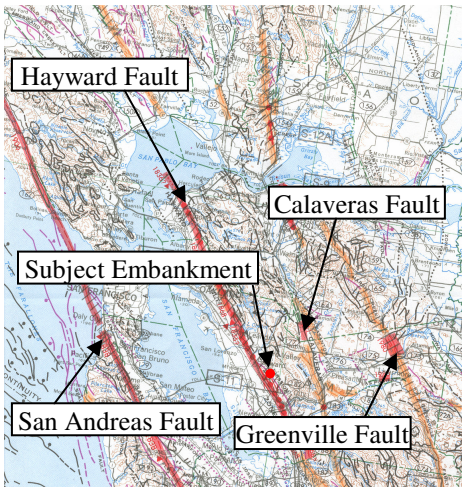

Figure 1. Regional fault map (after Jennings, 1994)

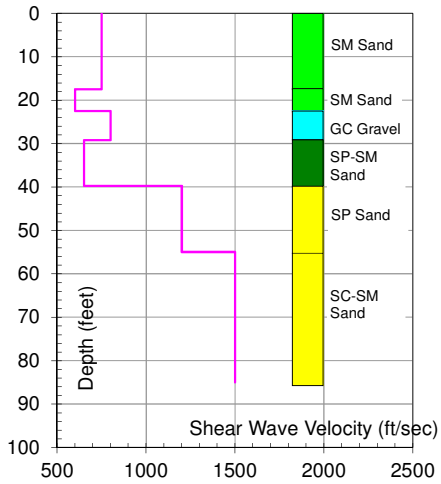

Figure 2. Generalized soil profile and estimated shear wave velocity

SITE SEISMICITY AND SELECTION OF INPUT GROUND MOTIONS

Input ground motions are usually selected and modified by scaling or matching to the target design response spectrum. Input ground motion selection is important because it has long been recognized that

the uncertainty in the ground motion characterization is the dominant source of uncertainty in evaluating seismic response of slopes or embankments (Bray and Travasarou, 2007).

Given the site's close distance, the Hayward Fault is considered the controlling seismic source. The target response spectrum was derived from a deterministic seismic hazard analysis (DSHA) using computer program EZ-FRISK (Risk Engineering, 2007). According to the guidelines recommended by Fraser and Howard (2002), a 50th percentile target response spectrum was determined associated with the following site characteristics: (1) a site-source distance of 0.81 miles; (2) a V_{s30} of about 900 ft/second. A design moment magnitude 7.3 was used based on the deaggregation of the DSHA.

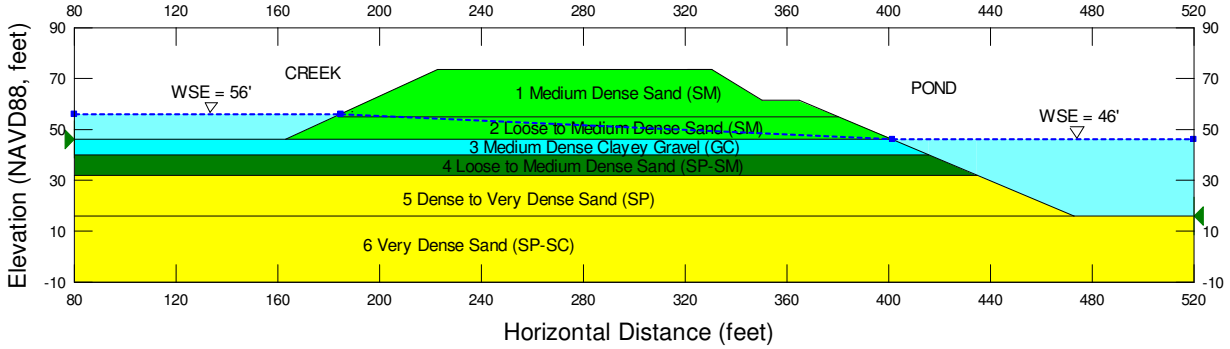

Figure 3. The generalized cross section

To date, there are no widely accepted standard procedures for selecting and modifying ground motions for use in dynamic analyses. In the current engineering state-of-practice, a "suitable" fit is the established rule of thumb that typically involves selection and simple scaling or spectral matching of ground motions to a target design response spectrum. However, there has not been any quantitative definition of "suitable" fit until a recent study by Kottke and Rathje (2008). In their study, they developed a semi-automated program, SigmaSpectra, which selects and scales sets of ground motions so that their mean matches a target design response spectrum. The program first matches the target spectral shape and then fits the amplitude and standard deviation of the target by adjusting the individual scale factors for the motions. The methodology employed by SigmaSpectra not only minimizes the root mean square error (RMSE) in log space between the target spectrum and the median response spectrum of the scaled suite of input ground motions, but also controls the standard deviation (σ_{ln}) of the scaled suite of input ground motions.

In this case study, a library of 173 ground motions was generated by searching the Next Generation Attenuation (NGA) strong motion database (http://peer.berkeley.edu/nga/search.html). The search criteria includes: (1) $6.5 < M_w < 8.0$; (2) 0 < source to site distance < 31 miles; (3) 600 feet/second < V_{s30} < 2500 feet/second; (4) strike-slip sources.

Following the determined target response spectrum, a number of suites comprising of various ground motions were derived using SigmaSpectra. In this study, suites comprising 3, 4, 5, 7, 10, 15, 20, 30, 50 ground motions were considered to examine the effect of the number of ground motions on the median RMSE and standard deviation RMSE (σ_{ln} RMSE) with the results presented in Figure 4.

As shown in Figure 4, the median RMSE first decreases and then increases with increasing the number of ground motions. The standard deviation RMSE continuously decreases with increasing the number of ground motions. For this case study, a suite of 7 ground motions was used for dynamic analyses. Figure 5 shows the suite of 7 motions selected and scaled to match the target response spectrum. Seven motions were selected from a large library of 173 ground motions with a median RMSE of 0.052.

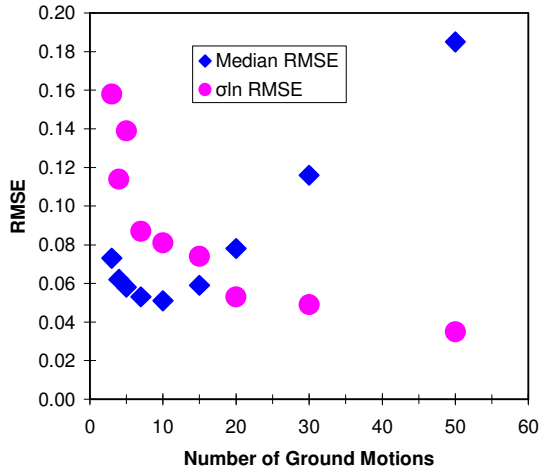

Figure 4. Fit parameters as a function of the number of motions for the 173-motion library

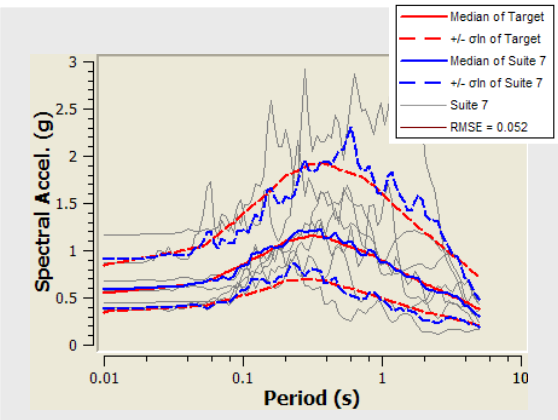

Figure 5. Response Spectra Median σ_{ln} of Suite of 7 Ground Motions

Table 1 presents details of the 7 selected ground motions. The scale factors for three of the seven selected ground motions are somewhat large compared to the typical range of scale factors used in engineering practice, and could be primarily attributed to the fact that not many ground motions recordings are available that have similar spectrum as the target spectrum.

Table 1. Selected Ground Motions

Station	Event	M_w	R (mi)	Scale Factor	Scaled PGA (g)
EL Centro Array #6	Imperial Valley, CA	6.5	2.2	1.98	0.87
EC Meloland OVERP FF	Imperial Valley, CA	6.5	2.2	2.30	0.68
Westmoreland Fire Sta	Imperial Valley, CA	6.5	9.6	5.39	0.40
OSA	Kobe, Japan	6.9	13.5	6.05	0.45
Istanbul	Kocaeli, Turkey	7.5	32	7.16	0.37
Yarimca	Kocaeli, Turkey	7.5	3.3	2.14	0.57
PTS	Superstition Hills, CA	6.5	2.2	2.66	1.17

NUMERICAL MODELING

Simplified Sliding Block Method

Seismic vulnerability evaluation of the embankment was carried out following the methodology that is presented in the companion paper (Liao et al., 2011). Prior to evaluating static slope stability of the embankment, a liquefaction triggering evaluation was conducted using the procedures proposed by Seed

et al. (2003). The results of the liquefaction analysis indicate that liquefiable silty sand with gravel exists below the subject embankment. Undrained residual shear strengths ($S_{u,r}$) of the potentially liquefiable soils were estimated based on the 33rd percentile of the range suggested by Seed and Harder (1990) as shown in Figure 6. Table 2 presents the soil properties used in the static slope stability analysis.

Table 2. Soil Parameters Used for Slope Stability Analyses and Dynamic Analyses

Material No. in Figure 3	Soil Type	γ (pcf)	φ' (°)	c' (psf)	$S_{u,r}^{*}$ (psf)	V_s^{**} (ft/s)	$G/G_{\max}$ Curve
1	Silty Sand (SM)	125	32	0	-	750	Seed & Idriss (1970, upper)
2 (7 for Liquefied)	Silty Sand (SM)	125	25	0	250	600	Seed & Idriss (1970, upper)
3	Clayey Gravel (GC)	125	26	50	1100	800	Seed & Idriss (1970, average)
4	Sand (SP-SM)	125	24	0	500	650	Seed & Idriss (1970, average)
5	Sand (SP)	125	35	0	-	1200	Seed & Idriss (1970, lower)
6	Sand (SP-SC)	125	40	200	-	1500	Seed & Idriss (1970, upper)

* The smaller value between $S_{u,r}$ and drained strength (φ', c') should be used for the simplified sliding block analysis.

**The small strain shear modulus was calculated as $G_{\max} = \rho V_s^2$, ρ is mass density.

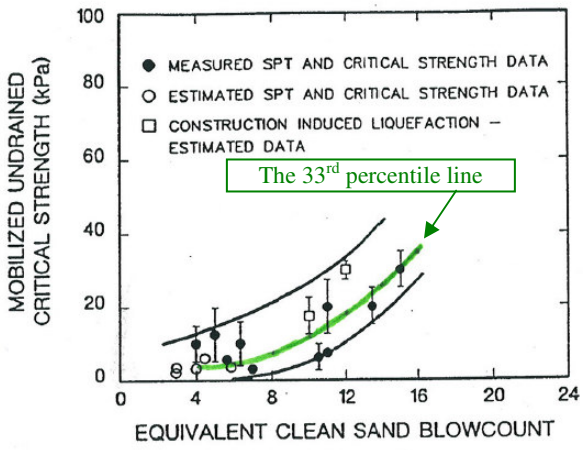

Figure 6. Recommended correlation between $S_{u,r}$ and $(N_1)_{60\text{-}cs}$ (Seed and Harder, 1990)

The static slope stability analyses were performed using the limit-equilibrium-based computer program SLOPE/W (Geo-Slope, 2008). Two scenarios were considered regarding the onset of the liquefaction with respect to the duration of the strong earthquake shaking. In the first scenario, liquefaction was assumed to start at the end of the shaking (i.e. no seismic inertial force). In this case, if factor of safety is less than 1.0, then the slope would likely be subjected to a flow failure. If the factor of safety is greater than 1.0 in the first scenario, then a second scenario was considered that assumes the possible onset of liquefaction during earthquake shaking. The second scenario implies that inertial loading would need to be applied in the slope stability analysis. For this case, a yield acceleration (k_y) was estimated and then compared to the design PGA. A k_y smaller than one quarter of the PGA may cause deformation on the order of more than 3 feet during the design earthquake using a simplified Newmark approach as presented

by Ambreseys and Menu (1988) and is consistent with Makdisi and Seed (1978). If the computed factor of safety in the first scenario is greater than 1.0 or the calculated k_y in the second scenario is larger than one quarter of the PGA, a lateral displacement should be estimated using the Bray and Travasarou procedure.

Fully Nonlinear Dynamic Analysis

In this case study, computer program FLAC was used to perform nonlinear dynamic analyses. Soils susceptible to liquefaction were modeled with the built-in Finn/Byrne constitutive model (Byrne, 1991). The Finn/Byrne model is an effective stress shear-volume coupling scheme that can simulate some important mechanisms of liquefaction (FLAC, 2008b). Non-liquefiable soils were modeled as Mohr-Coulomb materials with shear modulus degradation as described below.

For each soil material, modulus degradation and hysteric damping were implemented as a supplemental to either Finn/Byrne model or Mohr-Coulomb model to capture soil non-linearity and energy dissipation at large cyclic strain levels. Table 2 presents the hysteric damping curves used. In addition, a small amount of stiffness-proportional Rayleigh damping was added to account for damping at small strain levels.

The bottom boundary of the FLAC model was simulated as a quiet (viscous) boundary (Lysmer and Kuhlemeyer, 1969) to absorb the energy of body waves approaching the bottom boundary. A velocity time history converted from an acceleration time history is applied along the bottom boundary of the FLAC model as the input motion. The boundary conditions along the sides of the FLAC model were simulated using the free field boundary tool built into FLAC.

RESULTS AND DISCUSSIONS

Results of Simplified Sliding Block Analyses

Figure 7 presents the results of the post-liquefaction slope stability analyses with two potential sliding masses marked by the black bold lines. Critical wedge-shaped failure surfaces developed on both the creek and pond side slopes due to the liquefied soils (represented by red zones). The calculated factors of safety (FOS) for the creek and pond side slopes are 0.74 and 1.06, respectively, without applying any seismic coefficient, indicating that the creek side slope would be subjected to flow failure and the pond side slope would be marginally stable if the onset of the liquefaction occurs after seismic shaking. The k_y was calculated to be very small (< 0.02g) for the pond side slope, compared to the PGA (PGA = 0.59g in this case study). Because the calculated k_y is significantly less than one quarter of the PGA, a potential large lateral deformation for the pond side slope would likely be occur. Note that no lateral displacement was estimated using the Bray and Travasarou (2007) procedure due to the significant strength loss from liquefaction occurred.

The results of the simplified sliding block analysis indicate that both slopes are highly likely to be subjected to flow failures or large lateral movements. Magnitudes of potential lateral movements cannot be estimated using this analysis.

Results of Fully Nonlinear Dynamic Analysis

Example results of a FLAC dynamic analysis are presented in Figures 8 through 11 from runs performed using the acceleration time history recorded at Westmoreland Fire Station during the 1979 Imperial

Valley earthquake (see Table 1). Figure 8 presents the contours of horizontal displacements (X displacements in the contour plot). As shown in Figure 8, movements of the embankment after 10 seconds are primarily concentrated along the creek side slope and the pond side slope with the maximum displacement of approximately 2 feet. The central portion of the crest of the embankment which is about 1/3 of the entire width of the crest was subjected to a movement of less than 0.5 feet in both horizontal and vertical directions. Therefore, there would likely not be a significant freeboard loss under the design seismic event. Due to the relatively dense foundation soils, lateral movements are constrained primarily within the embankment.

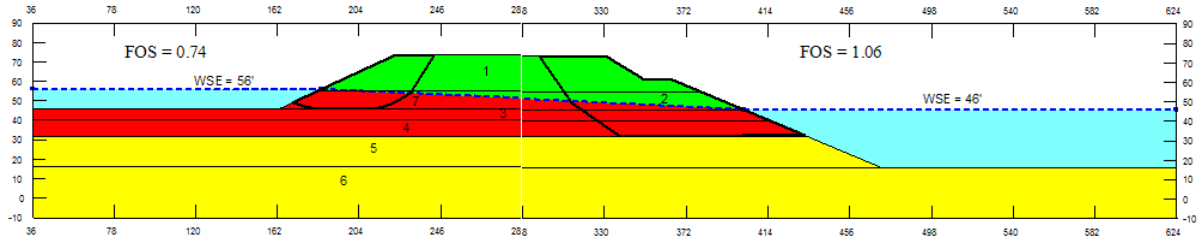

Figure 7. Results of post-liquefaction static slope stability analyses (first scenario) without seismic force

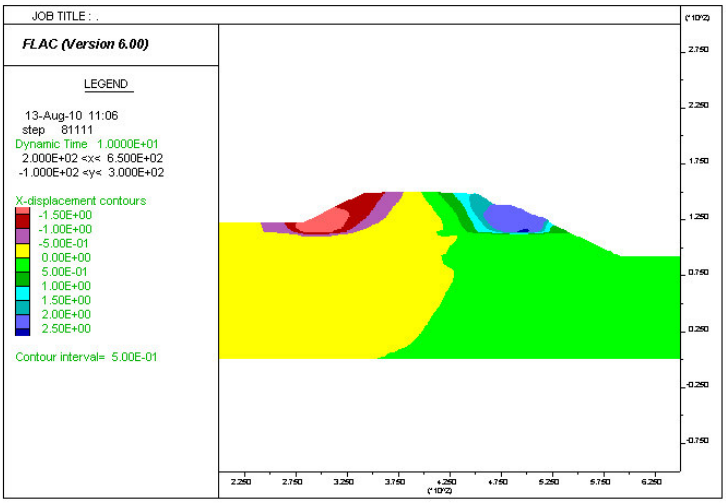

Figure 8. Contours of horizontal (x) displacements at 10 seconds (Westmoreland Fire Station, 1979 Imperial Valley Earthquake)

Contours of the maximum shear strain increment developed within the embankment and foundation are shown in Figure 9. As shown in Figure 9, the developed maximum shear strain within shearing zones was about 10 to 12%. A localized shear zone with maximum shear strains of 15 to 20 % was seen along the bottom of the pond side slip surface. The majority of the foundation soil was subjected to only a maximum shear strain of less than 1%.

Figure 10 presents the calculated horizontal (X) and vertical (Y) displacements. Trace number 815 represents the horizontal displacement calculated at the creek side crest hinge point while trace number 816 represents the vertical displacement calculated at the same location. Trace number 825 represents the

horizontal displacement calculated at the pond side crest hinge point while trace number 826 represents the vertical displacement calculated at the same location.

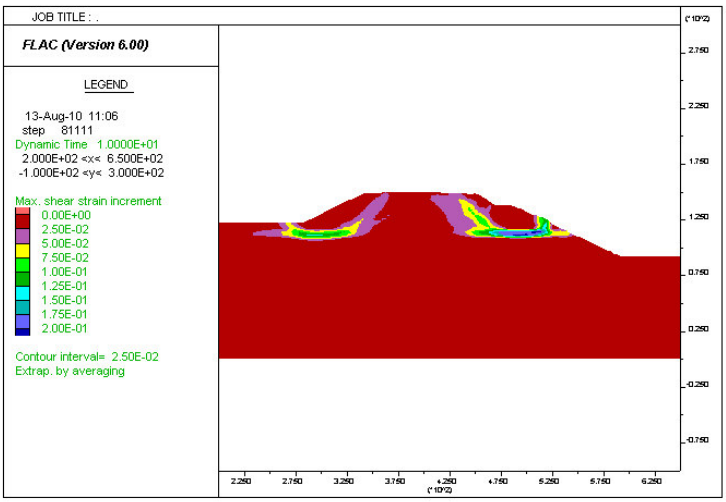

Figure 9. Maximum shear strain increment contours at 26 seconds (Westmoreland Fire Station, 1979 Imperial Valley Earthquake)

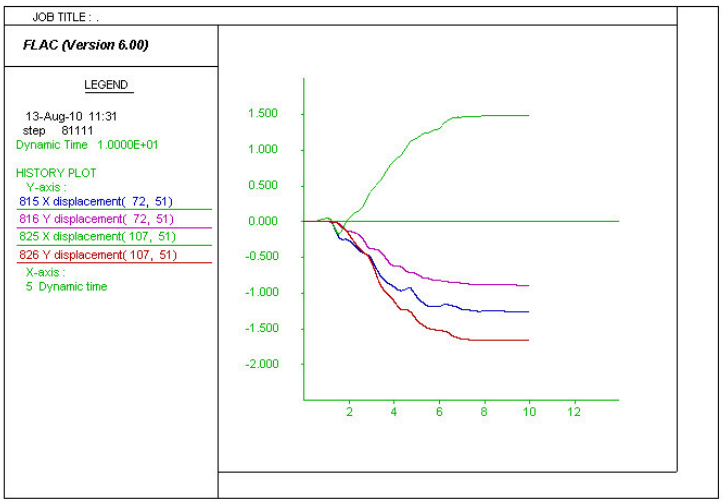

Figure 10. Comparisons of the input acceleration to the calculated horizontal (x) accelerations (Westmoreland Fire Station, 1979 Imperial Valley Earthquake)

Figure 11 presents two traces of excess pore pressure ratios (r_u) at grid point (83, 43) within material no. 2 (silty sand), which is about 28 feet below the crest, and at grid point (90, 38) within material no. 4 (SP-SM sand), which is about 39 feet below the crest. As shown in Figure 11, the trace of excess pore pressure ratios at grid point (83, 43) reached its peak value approximately one second after the onset of seismic shaking, which followed the arrival of the first acceleration spike as shown in Figure 10. The trace of excess pore pressure ratios at grid point (90, 38) did not reach its peak value until about 5 seconds

after the onset of seismic shaking. Both traces indicated that soils at the two locations were liquefied due to seimic shaking.

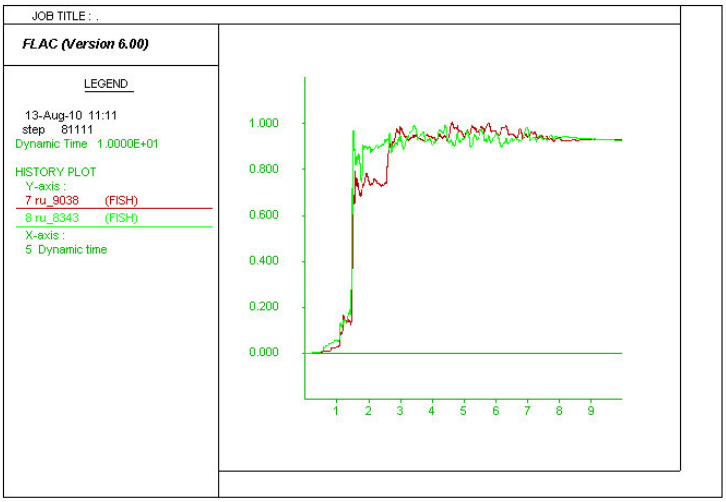

Figure 11. Traces of excess pore pressure ratios (Westmoreland Fire Station, 1979 Imperial Valley Earthquake)

A series of 7 dynamic analyses were carried out using the input ground motions contained in Table 1. In summary, results of the fully nonlinear dynamic analyses indicated that the potential lateral movements of the embankment could be from about 2 feet to 6 feet along the creek and pond side slopes. The central 1/3 of the crest of the embankment would likely be subjected to less than 0.5 feet movement both horizontally and vertically. There would likely be no significant freeboard loss during the design earthquake event. However, the embankment would likely require a repair to re-grade the crest to its original surface condition and geometry following the design seismic event.

DISCUSSIONS

Both the simplified sliding block analysis and the fully nonlinear dynamic analysis predicted approximately very similar failure surfaces on both the creek and pond side slopes. However, results of the simplified sliding block analysis indicated that a potential flow failure (i.e., large lateral movements) would occur but the magnitude was not predicable either because the post-liquefaction factor of safety was smaller than 1.0 or the estimated k_y is too small (< 0.02g in this case study). The difficulty of using the simplified sliding block analysis to predict the magnitude of the lateral movement can be attributed to the relatively significant strength losses of liquefied soils.

On the other hand, the fully nonlinear dynamic analysis predicted not only the occurrence of the liquefaction that agrees well with that using the simplified liquefaction procedures (Seed et al., 2003), but also the magnitudes of the potential lateral movements. The Finn/Byrne model built into the FLAC model for liquefiable soils simulates well the main mechanism of liquefaction.

CONCLUSIONS

A case study has been presented that illustrates two approaches to evaluate seismic vulnerability of an embankment located in the highly seismically active San Francisco Bay Area. The results of our analyses indicated that lateral movements of about 2 feet to 6 feet should be anticipated along two slopes during the design seismic event due to the soil liquefaction within the embankment fill. The central 1/3 of the crest of the embankment would likely be subjected to less than 0.5 feet movement both horizontally and vertically. There would likely be no significant freeboard loss during the design earthquake event. However, the embankment would likely require a repair to re-grade the crest to its original surface condition and geometry following the design seismic event.

ACKNOWLEDGEMENTS

The authors would like to appreciate Mr. James Gingery of Kleinfelder for his thoughtful review and helpful comments on this paper.

REFERENCES

Ambraseys, N. N., and Menu, J. M. (1988). "Earthquake-Induced Ground Displacements", Journal of Earthquake Engineering and Structural Dynamics, 16, pp. 985–1006.

Ausilio, E., Costanzo, A., and Tropeano, G. (2009). "Evaluation of Seismic Displacements of A Natural Slope by Simplified Methods and Dynamic Analyses", in Proceedings of Performance-Based Design in Earthquake Geotechnical Engineering, Japan, pp. 955-962.

Beaty, M. H., and Byrne, P. (2000). "A Synthesized Approach for Predicting Liquefaction and Resulting Displacements", in Proceedings of the Twelve World Conference on Earthquake Engineering, Auckland, New Zealand, Paper No. 1589, Jan. 30 - Feb. 4, 2000.

Bray, J. D., and Travasarou, T. (2007). "Simplified Procedure for Estimating Earthquake-induced Deviatoric Slope Displacements", Journal of Geotechnical and Geoenvironmental Engineering, Vol. 133(4), pp. 381–392.

Byrne, P. M. (1991). "A Cyclic Shear-Volume Coupling and Pore-Pressure Model for Sand", in Proceedings of Second International Conference on Recent Advances in Geotechnical Earthquake Enginering and Soil Dynamics, St. Louis, Missouri, Paper No. 1.24, pp. 47 - 55.

Byrne, P. M., Debasis, R., Campanella, R. G., and Hughes, J. (1995). "Predicting Liquefaction Response of Granular Soils from Self-Boring Pressuremeter Tests", ASCE National Convention, San Diego, California, Oct. 23 – 27, ASCE 56 (GSP), pp 122 – 135.

Fraser, W. A., and Howard, J. K. (2002). "Guidelines for use of the Consequence-Hazard Matrix and Selection of Ground Motion Parameters", the Resources Agency, Department of Water Resources, Division of Safety of Dams, California.

GEO-SLOPE International Ltd. (2008). Stability Modeling with SLOPE/W 2007 Version, 4th Edition, Calgary, Alberta, Canada.

Ishihara, K. (1984). "Post-Earthquake Failure of A Tailing Dam due to Liquefaction of the Pond Deposit", in Proceedings of International Conference on Case Histories in Geotechnical Engineering, Rolla, Missouri, Vol. 3, pp. 1129-1143.

Itasca Consulting Group. (2008a). FLAC, Fast lagrangian analysis of continua, user's guide, Minneapolis, Minnesota, USA.

Itasca Consulting Group. (2008b). FLAC, Fast lagrangian analysis of continua, Dynamic Analysis, Minneapolis, Minnesota, USA.

Jennings, C.W. (1994). Fault Activity Map of California and Adjacent Areas with Locations and Ages of Recent Volcanic Eruptions, California Division of Mines and Geology.

Kottke, A., and Rathje, A. M. (2008). "A Semi-Automated Procedure for Selection and Scaling of Recorded Earthquake Motions for Dynamic Analysis", Earthquake Spectra, 24(4), pp. 911 – 932.

Liao, J., Zafir, Z., and Anderson, S. (2011). "Development of a Methodology for Estimating Simplified Seismic Slope Deformation of Levees with Seepage Mitigations", in Proceedings of the 5th International Conference on Earthquake Geotechnical Engineering, Santiago, Chile, Jan. 10 – 13, 2011.

Lin, J-S, and Whitman, R. (1986). "Earthquake Induced Displacements of Sliding Blocks", Journal of Geotechnical Engineering Vol. 112(1), pp. 44–59.

Lysmter, J., and Kuhlemeyer, R. L. (1969). "Finite Dynamic Model for Infinite Media", Journal of Engineering Mechanics, 95(EM4), pp. 859-877.

Makdisi, F, and Seed, H. B. (1978). "Simplified Procedure for Estimating Dam and Embankment Earthquake Induced Deformations", Journal of Geotechnical Engineering, Vol. 104(7), pp. 849–867.

Newmark, N. M. (1965). "Effects of Earthquakes on Dams and Embankments", Geotechnique, London, 15(2), pp. 139–160.

Risk Engineering. (2005). EZ-FRSIK, Version 7.20, http://www.riskeng.com

Olson, S. M., and Johnson, C. I. (2008). "Analyzing Liquefaction-Induced Lateral Spreads Using Strength Ratios", Journal of Geotechnical and Geoenvironmental Engineerig, Vol. 134, No. 8. Pp. 1035 – 1049.

Pacific Earthquake Engineering Center (PEER), http://peer.berkeley.edu/nga/search.html

Seed, H. B. (1987). "Design Problems in Soil Liquefaction", Journal of Geotechnical Engineering, Vol. 113 (8), pp. 827-845.

Seed, R. B. et al. (2003). "Recent Advances in Soil Liquefaction Engineering: a Unified and Consistent Framework", Keynote presentation, 26th Annual ASCE Los Angeles Geotechnical Spring Seminar, Long Beach, CA.

Seed, R. B, and Harder, L. F. (1990). "SPT-Based Analysis of Cyclic Pore Pressure Generation and Undrained Residual Shear Strength", in Proceedings of the H.B. Seed Memorial Symposium, Bi-Tech Publishing Ltd., Vol. 2, pp. 351-376.

Seed, H. B., and Idriss, I. M. (1970). "Soil Moduli and Damping Factors for Dynamic Response Analysis", Earthquake Engineering Research Center, University of California, Berkeley, Report No. UCB/EERC-70/10, p 48.

Working Group on California Earthquake Probabilities (WGCEP). (2007). The Uniform California Earthquake Rupture Forecast, Version 2, U.S. Geological Survey, Open File Report 2007 – 1437.

Yegian, M. et al. (1991). "Seismic Risk Analysis for Earth Dams", Journal of Geotechnical Engineering, Vol. 117(1), pp. 35–50.